Single-Molecule Detection of a Fluorescent Nucleobase Analog via Multiphoton Excitation

David Nobis,[1,‡] Rachel S. Fisher,[2,‡] Mats Simmermacher,[2] Patrycja A. Hopkins,[3] Yitzhak Tor,[3] Anita C. Jones,[2,*] and Steven W. Magennis[1,*]

[1] WestCHEM School of Chemistry, University of Glasgow, Joseph Black Building, University Avenue, Glasgow, G12 8QQ, UK

[2] EaStCHEM School of Chemistry, The University of Edinburgh, West Mains Road, Edinburgh, EH9 3JJ, UK

[3] Department of Chemistry and Biochemistry, University of California, San Diego, 9500 Gilman Drive, La Jolla, CA 92093 USA

Supporting Information Placeholder

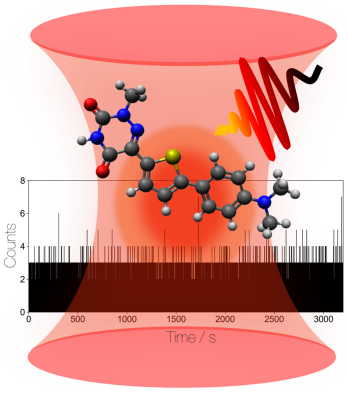

ABSTRACT: The ability to routinely detect fluorescent analogs of nucleobases at the single-molecule level would create a wealth of opportunities to study nucleic acids. We report the multiphoton-induced fluorescence and single-molecule detection of a dimethylamine-substituted extended-6-aza-uridine (**DMAthaU**). We show that **DMAthaU** can exist in a highly fluorescent form, emitting strongly in the visible region (470–560 nm). Using pulse-shaped broadband Ti:sapphire laser excitation, **DMAthaU** undergoes two-photon (2P) absorption at low excitation powers, switching to three-photon (3P) absorption at high incident intensity. The assignment of a 3P process is supported by cubic response calculations. Under both 2P and 3P excitation, the single-molecule brightness was over an order of magnitude higher than reported previously for any fluorescent base analog, which facilitated the first single-molecule detection of an emissive nucleoside with multiphoton excitation.

Fluorescence-based methods are powerful tools for studying the structure, dynamics and interactions of nucleic acids *in vitro* and *in vivo*, and for technologies such as DNA sequencing and high-throughput screening. These methods typically involve covalent attachment of large fluorescent dyes via long linkers, but such labels are insensitive to local base interactions and may also perturb native interactions (*e.g.* with proteins).[1] Fluorescent base analogs (FBA) that preserve native nucleic acid structure can address such limitations,[2-10] but these have not yet found application in ultrasensitive analysis.[11-13] The main reasons for this are lower absorption cross section (ε) than extrinsic dyes, limiting their brightness ($\varepsilon\phi$, where ϕ is the emission quantum yield); short (UV) absorption wavelength, leading to photobleaching and poorer optical penetration into biological media.

A possible way to overcome these limitations is multiphoton excitation,[14-19] with potential benefits including deeper penetration into tissue in the near-IR, 3D control of excitation, and reduction of photobleaching and background fluorescence.[20-21] With the aim of reaching the ultimate single-molecule level of detection, we recently reported that an adenine analog, pA, incorporated into single-stranded oligonucleotides could undergo two-photon (2P) excitation[22] and as few as 5 molecules could be detected.[23] Moreover, pA had enhanced photostability under 2P excitation. This demonstrated the feasibility of single-molecule detection, albeit improvements in brightness were still required.[23]

Here we demonstrate that an extended 6-aza-uridine ribonucleoside, **DMAthaU** (Chart 1), adopts a highly fluorescent form, in which the brightness following three-photon (3P) excitation is over an order of magnitude greater than that of pA under 2P excitation, allowing, for the first time, single-molecule detection via multiphoton excitation.

Chart 1. Rotameric and tautomeric structures of the extended thiophene-6-aza-uridine, DMAthaU.

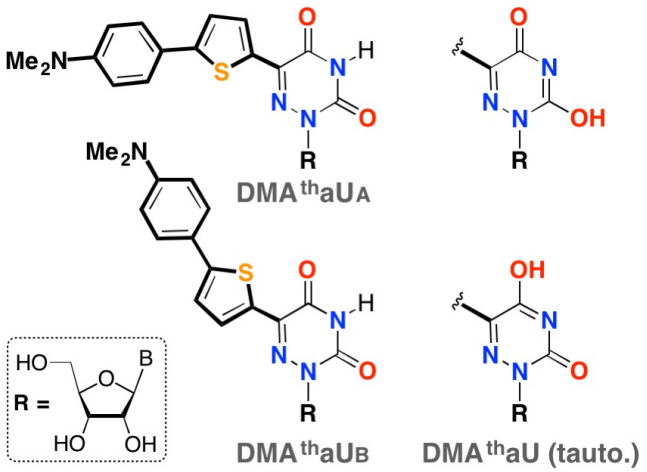

DMAthaU is a member of a family of tuneable fluorescent 6-aza-uridines, the synthesis of which was reported previously.[24] Herein, we performed ensemble spectroscopic studies for **DMAthaU** in either aqueous Tris buffer or dioxane. In buffer, the absorption maximum is at 385 nm while the excitation peak is blueshifted to around 330 nm (Fig. S1). The emission maximum is at 440 nm (Fig. S2). The discrepancy between the excitation and absorption spectra indicates the presence of a dark (non-emissive) species, absorbing at longer wavelengths. This is confirmed by a strong dependence of the steady-state quantum yield (the average over all absorbing species) on the excitation wavelength (Table S1). The quantum yield (ϕ) decreases from 0.05 to 0.003 on shifting the excitation wavelength from 330 nm to 380 nm. In dioxane, in contrast, the absorption and excitation spectra are identical (Fig. S3), and coincide with the absorption spectrum in buffer. As reported previously,[24] the fluorescence of **DMAthaU** is responsive and dependent on solvent polarity; its emission spectrum in dioxane is red-shifted relative to that in buffer, and ϕ is increased to 0.20.

Fluorescence decays of **DMAthaU** were recorded in buffer (Fig. S4 and Tables S2 and S3) at three excitation wavelengths (364, 380 and 400 nm); these could be fitted globally to three decay components with common lifetimes of 0.19, 1.3 and 5.9 ns, respectively, but showed a marked dependence of A factors on excitation wavelength (Table S3). This results in a decrease in the average lifetime from 2.2 ns to 0.60 ns, on increasing the excitation wavelength from 360 to 400 nm. However, the decrease in average lifetime is not commensurate with the decrease in quantum yield, indicating the excitation of dark states at longer wavelengths. Further evidence of dark states comes from comparison of the average lifetimes and quantum yields in buffer and dioxane. In dioxane, an average lifetime of 1.8 ns (Table S4) corresponds to a quantum yield of 0.2, whereas in buffer, a $\langle\tau\rangle$ value of 2.2 ns (excitation at 380 nm) corresponds to a ϕ of 0.003. On the basis of these values, assuming no dark states in dioxane, we estimate that 96% of the population excited at 380 nm in buffer is non-emissive (see SI for details).

It is evident from the ensemble measurements that, in Tris buffer, **DMAthaU** exists in at least three emissive states and at least one dark state. This photophysical complexity is perhaps unsurprising given that **DMAthaU** can populate two distinct rotamers (with relative rotation of the azauridine and thiophene rings by 180°) and three tautomers, as illustrated in Chart 1. Ground-state density functional theory (DFT) calculations, in the gas phase and within a solvent continuum, show that the molecule exists preferentially as rotamer A (Chart 1), with rapid (ns) interconversion between rotamers; [25] In contrast, the three tautomers of the core 6-aza-uracil heterocycle have been shown to interconvert on much longer timescales (μs–ms).[26] Although the ensemble-average quantum yield of **DMAthaU** in buffer is much less than in dioxane, two of its emitting species have longer lifetimes, and hence higher individual quantum yields, than found in dioxane. We estimate that the longest lifetime species in buffer has an emission quantum yield of about 0.6.

Multiphoton excitation was first investigated in dioxane in ensemble measurements. The emission resulting from IR excitation (Fig S3) is attributed to a 2P process, based on the dependence of the emission intensity on laser power (Fig. S5); the log–log plot following excitation at 840 nm has a slope of 1.85 ± 0.04. Since 2P excitation results in the same emission spectrum as that seen for one-photon (1P) excitation (Fig S3), the emission is dominated by the same species in each instance. The 2P cross-section (σ_2) of **DMAthaU** in dioxane, measured relative to rhodamine 6G, is 90.0 ± 5.0 GM with a corresponding 2P brightness of 18 GM. This cross-section is higher than that of any other FBA studied previously, including pA (21 GM in ethanol[23]) and the brightness is three times greater than that of pA.

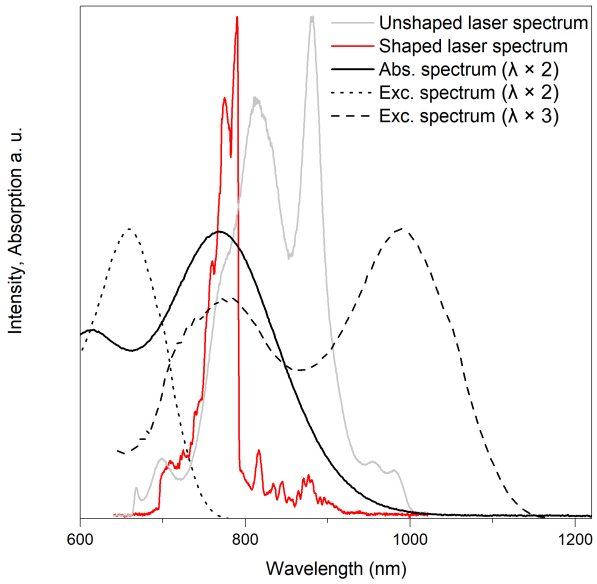

Figure 1. The laser excitation profiles, unshaped (grey line) and pulse-shaped (red line), are compared with the **DMAthaU** one-photon absorption spectrum (black line, plotted against double the one-photon wavelength), and the one-photon excitation spectrum plotted against double (dotted line) and triple (dashed line) the one-photon wavelength.

Given the existence of **DMAthaU** in a highly fluorescent state (albeit with a low population) we were encouraged to pursue single-molecule detection in buffer. The multiphoton excitation of **DMAthaU** in buffer was investigated using a home-built microscope with broadband femtosecond laser excitation and photon-counting detection.[23] Measurement and compensation for dispersion in the optical system[27] is achieved by dual amplitude- and phase-shaping of the laser pulse, using multiphoton intra-pulse interference phase scan (MIIPS).[28] The spectral width and center of the laser spectrum were varied to optimize the signal-to-background ratio (SBR, Fig. S6). This improved the SBR by a factor of 1.5 (Fig. 1).

The power-dependence for a solution of **DMAthaU** in buffer (Fig. 2) is rather different to that measured in dioxane (Fig. S5). At low powers, the curve has a slope of ~2, which switches at higher powers to a slope of ~3, indicative of 3P absorption. At the highest laser powers, saturation occurs. As discussed above, the 1P excitation maximum is blue-shifted with respect to the absorption peak (Fig. S1), so the excitation maximum at twice the 1P wavelength has a weak overlap with the laser spectrum (Fig. 1). In contrast, tripling the 1P excitation wavelength gives a very good match to the laser spectrum, particularly with the optimized pulse (Fig. 1). The decay parameters measured in either the 2P or 3P excitation regimes are essentially identical (considering the excitation-wavelength dependence) to those for 1P excitation, confirming that the emission originates from the same excited states in each case (Fig. S7).

In support of the assignment of 3P excitation, we performed cubic response calculations within time-dependent density functional theory (TDDFT) for the two optimized rotamer structures (Fig. S8). The key finding (Table 1) is that for both rotamers there are particularly strong 3P transitions (the fifth and sixth) that display degenerate 3P absorption wavelengths close to the maximum of the optimized laser spectrum (Fig. 1). Furthermore, the magnitude of the calculated 3P cross sections are in agreement with estimated 3P cross sections[29] and those measured for fluorophores of similar size.[30]

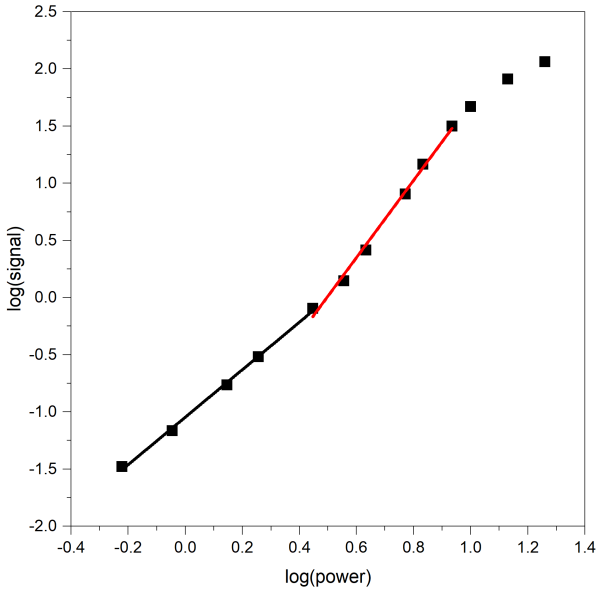

Figure 2. Power-dependence of **DMAthaU** emission intensity in buffer. The lower part of the curve (pulse energy <35 pJ) was fitted with a slope of 2.1 (black line). At higher powers (pulse energy 35-107 pJ), the slope is 3.3 (red line).

Table 1. Degenerate three-photon absorption wavelengths λ^{3PA} in nm and three-photon absorption cross-sections σ^{3PA} in 10^{-82} cm^6 s^2 photon^{-2} for the first ten transitions from the electronic ground states of two rotamers DMAthaU_A and DMAthaU_B. [a]

	DMAthaU_A		DMAthaU_B	
	λ^{3PA}	σ^{3PA}	λ^{3PA}	σ^{3PA}
1	1110	59.9	1120	67.4
2	834	100	838	22.4
3	825	0.457	827	18.0
4	818	7.90	816	38.4
5	790	1,940	785	10,800
6	769	12,500	777	3,590
7	695	5.98	698	6.94
8	680	48.0	683	64.5

9	655	65.8	657	97.0
10	648	13.9	647	7.26

[a]The values are calculated with CAM-B3LYP/cc-pVDZ for linearly polarised light and nuclear geometries optimized with B3LYP/cc-pVTZ (see SI and refs. 31-39).

Next, we examined the limits of detection of **DMAthaU** in buffer, using fluorescence correlation spectroscopy (FCS) and photon-counting with a multichannel scaler (MCS), similar to our recent work with pA.[23] Excitation powers of 10 mW, where the 3P excitation begins to saturate, gave the best SBR; the pulses were compressed to 8 fs at the focal plane.

In FCS measurements there was a striking discrepancy between the known sample concentration and the number of molecules observed in the laser focus. The correlation curve in Fig. 3 was recorded for a 525-nM solution, as determined by UV-Vis absorption.[24] On average ~0.4 molecules were found in the focus at this concentration. In contrast, for Rh110 at 10 nM there were ~1.4 molecules in the focus. Assuming all of the Rh110 molecules are detected, this implies that ~1/180 of the **DMAthaU** molecules that go through the focus are emissive, which agrees with the finding from bulk measurements that ~96% of the molecules are in a dark state. Based on the discussion above, and previous reports of tautomerism of FBAs,[40-42] we assign this dark state to a long-lived tautomer of **DMAthaU**.[26]

The diffusion time of **DMAthaU** is 25 µs, which is commensurate with the size of the freely-diffusing ribonucleoside, and is independent of the sample concentration. The number of detected molecules scales linearly with concentration (Fig. S9). For those **DMAthaU** molecules in the bright state, the single-molecule brightness, as given by the count rate per molecule (CPM), is 6.9 ± 0.2 kHz / molecule, over an order of magnitude higher than for pA.[23]

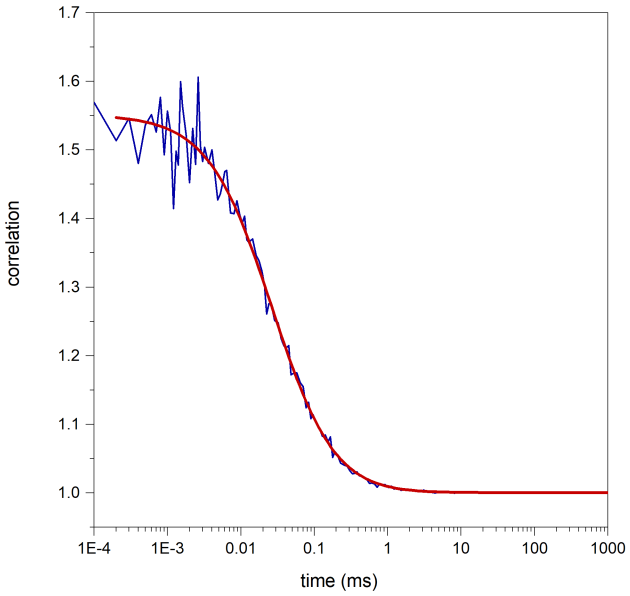

Figure 3. FCS curve of **DMAthaU** in buffer at pH 7.7. The blue line depicts the data and the fit is shown in red for a single-emitting species undergoing diffusion in a 3D Gaussian volume. The number of molecules in the focus is 0.5.

The high brightness of **DMAthaU** determined by FCS motivated us to attempt single-molecule detection. An MCS trace was recorded for a dilute solution (~10^{-11} M of bright **DMAthaU** molecules) (Fig. 4a) and compared to a measurement of pure buffer (Fig. 4b). Single molecules of **DMAthaU** are clearly identified as short-lived (ms) bursts on the background (see Fig. S10 for a detailed burst analysis). Although the bursts are small, their magnitude agrees with the CPM derived from FCS (note that the CPM for the sample in Fig. 4 is closer to 5 kHz / molecule due to the presence of an additional filter to further optimise the SBR).

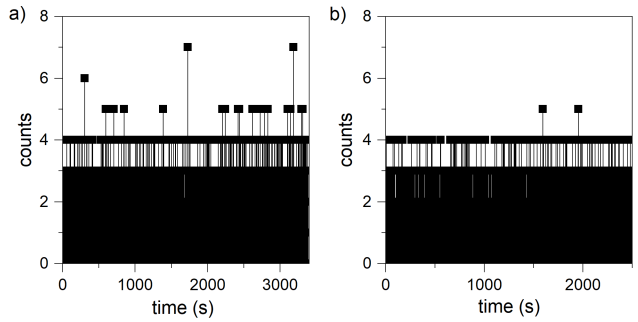

Figure 4. Single-molecule traces with laser power corresponding to the 3P regime for a) **DMAthaU** diluted in buffer (1x10^{-11} M of bright molecules) and b) buffer only.

In conclusion, we have shown for the first time that an FBA, an extended 6-aza-uridine ribonucleoside (**DMAthaU**), can be detected at the single-molecule level using multiphoton excitation. This highly fluorescent species is a monomer of **DMAthaU**, which undergoes 3P excitation at ~800 nm, as supported by TDDFT calculations. Future studies will focus on incorporating **DMAthaU** into DNA and RNA. It will be particularly interesting to see which species are present in DNA/RNA and how the presence of neighbouring bases influences the brightness of **DMAthaU**. In this context, the quantum yield in dioxane suggests that we may have additional enhancements in brightness due to changes in the local environment upon incorporation in an oligonucleotide. The potential for unprecedented insight into the mechanism of processes involving nucleic acids at the individual base level may soon be realised.

ASSOCIATED CONTENT

Supporting Information.

The Supporting Information is available free of charge on the ACS Publications website. A PDF of supplementary methods, Figures S1–10 and Tables S1–4.

AUTHOR INFORMATION

Corresponding Author

*E-mail: a.c.jones@ed.ac.uk (ACJ) or steven.magennis@glasgow.ac.uk (SWM)

Author Contributions

‡These authors contributed equally.

Funding Sources

No competing financial interests have been declared.

ACKNOWLEDGMENT

This work was supported by EPSRC (studentships for DN and RSF) and the University of Edinburgh (RSF). We thank the National Institutes of Health for generous support (via grant number GM 069773).

REFERENCES

1. Stennett, E. M. S.; Ciuba, M. A.; Lin, S.; Levitus, M., Demystifying PIFE: The Photophysics Behind the Protein-Induced Fluorescence Enhancement Phenomenon in Cy3. *J. Phys. Chem. Lett.* **2015,** *6*, 1819-1823.
2. Wilhelmsson, L. M., Fluorescent Nucleic Acid Base Analogues. *Q. Rev. Biophys.* **2010,** *43*, 159-183.
3. Sinkeldam, R. W.; Greco, N. J.; Tor, Y., Fluorescent Analogs of Biomolecular Building Blocks: Design, Properties, and Applications. *Chem. Rev.* **2010,** *110*, 2579-2619.
4. Xu, W.; Chan, K. M.; Kool, E. T., Fluorescent Nucleobases as Tools for Studying DNA and RNA. *Nature Chem.* **2017,** *9*, 1043-1055.
5. Burns, D. D.; Teppang, K. L.; Lee, R. W.; Lokensgard, M. E.; Purse, B. W., Fluorescence Turn-On Sensing of DNA Duplex Formation by a Tricyclic Cytidine Analogue. *J. Am. Chem. Soc.* **2017,** *139*, 1372-1375.
6. Shin, D.; Sinkeldam, R. W.; Tor, Y., Emissive RNA Alphabet. *J. Am. Chem. Soc.* **2011,** *133*, 14912-14915.
7. Rovira, A. R.; Fin, A.; Tor, Y., Chemical Mutagenesis of an Emissive RNA Alphabet. *J. Am. Chem. Soc.* **2015,** *137*, 14602-14605.
8. Wranne, M. S.; Fuchtbauer, A. F.; Dumat, B.; Bood, M.; El-Sagheer, A. H.; Brown, T.; Graden, H.; Grotli, M.; Wilhelmsson, L. M., Toward Complete Sequence Flexibility of Nucleic Acid Base Analogue FRET. *J. Am. Chem. Soc.* **2017,** *139*, 9271-9280.
9. Han, J. H.; Yamamoto, S.; Park, S.; Sugiyama, H., Development of a Vivid FRET System Based on a Highly Emissive dG-dC Analogue Pair. *Chem. Eur. J.* **2017,** *23*, 7607-7613.
10. Jones, A. C.; Neely, R. K., 2-Aminopurine as a Fluorescent Probe of DNA Conformation and the DNA-Enzyme Interface. *Q. Rev. Biophys.* **2015,** *48*, 244-279.
11. Wennmalm, S.; Blom, H.; Wallerman, L.; Rigler, R., UV-Fluorescence Correlation Spectroscopy of 2-Aminopurine. *Biol. Chem.* **2001,** *382*, 393-397.
12. Sanabia, J. E.; Goldner, L. S.; Lacaze, P. A.; Hawkins, M. E., On the Feasibility of Single-Molecule Detection of the Guanosine-Analogue 3-MI. *J. Phys. Chem. B* **2004,** *108*, 15293-15300.
13. Aleman, E. A.; de Silva, C.; Patrick, E. M.; Musier-Forsyth, K.; Rueda, D., Single-Molecule Fluorescence Using Nucleotide Analogs: A Proof-of-Principle. *J. Phys. Chem. Lett.* **2014,** *5*, 777-781.
14. Katilius, E.; Woodbury, N. W., Multiphoton Excitation of Fluorescent DNA Base Analogs. *J. Biomed. Opt.* **2006,** *11*, 044004.
15. Stanley, R. J.; Hou, Z. J.; Yang, A. P.; Hawkins, M. E., The Two-Photon Excitation Coss Section of 6MAP, a Fluorescent Adenine Analogue. *J. Phys. Chem. B* **2005,** *109*, 3690-3695.
16. Lane, R. S. K.; Magennis, S. W., Two-Photon Excitation of the Fluorescent Nucleobase Analogues 2-AP and tC. *RSC Adv.* **2012,** *2*, 11397-11403.
17. Mikhaylov, A.; de Reguardati, S.; Pahapill, J.; Callis, P. R.; Kohler, B.; Rebane, A., Two-Photon Absorption Spectra of Fluorescent Isomorphic DNA Base Analogs. *Biomed. Opt. Express* **2018,** *9*, 447-452.
18. Lane, R. S. K.; Jones, R.; Sinkeldam, R. W.; Tor, Y.; Magennis, S. W., Two-Photon-Induced Fluorescence of Isomorphic Nucleobase Analogs. *ChemPhysChem* **2014,** *15*, 867-871.
19. Stoltzfus, C. R.; Rebane, A., Optimizing Ultrafast Illumination for Multiphoton-Excited Fluorescence Imaging. *Biomed. Opt. Express* **2016,** *7*, 1768-1782.
20. He, G. S.; Tan, L. S.; Zheng, Q.; Prasad, P. N., Multiphoton Absorbing Materials: Molecular Designs, Characterizations, and Applications. *Chem. Rev.* **2008,** *108*, 1245-1330.
21. Zipfel, W. R.; Williams, R. M.; Webb, W. W., Nonlinear Magic: Multiphoton Microscopy in the Biosciences. *Nat. Biotechnol.* **2003,** *21*, 1368-1376.
22. Bood, M.; Fuchtbauer, A. F.; Wranne, M. S.; Ro, J. J.; Sarangamath, S.; El-Sagheer, A. H.; Rupert, D. L. M.; Fisher, R. S.; Magennis, S. W.; Jones, A. C.; Hook, F.; Brown, T.; Kim, B. H.; Dahlen, A.; Wilhelmsson, L. M.; Grotli, M., Pentacyclic Adenine: a Versatile and Exceptionally Bright Fluorescent DNA Base Analogue. *Chem. Sci.* **2018,** *9*, 3494-3502.
23. Fisher, R. S.; Nobis, D.; Fuchtbauer, A. F.; Bood, M.; Grotli, M.; Wilhelmsson, L. M.; Jones, A. C.; Magennis, S. W., Pulse-Shaped Two-Photon Excitation of a Fluorescent Base Analogue Approaches Single-Molecule Sensitivity. *Phys. Chem. Chem. Phys.* **2018,** *20*, 28487-28498.
24. Hopkins, P. A.; Sinkeldam, R. W.; Tor, Y., Visibly Emissive and Responsive Extended 6-Aza-Uridines. *Org. Lett.* **2014,** *16*, 5290-5293.
25. Fisher, R. S. Photophysical Characterisation of Fluorescent Base Analogues. PhD, The University of Edinburgh, 2018.
26. Markova, N.; Pejov, L.; Enchev, V., A Hybrid Statistical Mechanics-Quantum Chemical Model for Proton Transfer in 5-Azauracil and 6-Azauracil in Water Solution. *Int. J. Quantum Chem* **2015,** *115*, 477-485.
27. Pastirk, I.; Dela Cruz, J. M.; Walowicz, K. A.; Lozovoy, V. V.; Dantus, M., Selective Two-Photon Microscopy with Shaped Femtosecond Pulses. *Opt. Express* **2003,** *11*, 1695-1701.
28. Lozovoy, V. V.; Pastirk, I.; Dantus, M., Multiphoton Intrapulse Interference. IV. Ultrashort Laser Pulse Spectral Phase Characterization and Compensation. *Opt. Lett.* **2004,** *29*, 775-777.
29. Xu, C.; Webb, W. W., *Multiphoton Excitation of Molecular Fluorophores and Nonlinear Laser Microscopy*. Plenum Press: New York, 1997; Vol. 5, p 471-540.
30. Shear, J. B.; Brown, E. B.; Webb, W. W., Multiphoton-Excited Fluorescence of Fluorogen-Labeled Neurotransmitters. *Anal. Chem.* **1996,** *68*, 1778-1783.
31. Jansik, B.; Sałek, P.; Jonsson, D.; Vahtras, O.; Ågren, H., Cubic Response Functions in Time-Dependent Density Functional Theory. *J. Chem. Phys.* **2005,** *122*, 054107.
32. Yanai, T.; Tew, D. P.; Handy, N. C., A New Hybrid Exchange-Correlation Functional using the Coulomb-Attenuating Method (CAM-B3LYP). *Chem. Phys. Lett.* **2004,** *393*, 51-57.
33. Dunning, T. H., Gaussian-Basis Sets For Use In Correlated Molecular Calculations. 1. The Atoms Boron Through Neon Ans Hydrogen. *J. Chem. Phys.* **1989,** *90*, 1007-1023.
34. Woon, D. E.; Dunning, T. H., Gaussian-Basis Sets For Use In Correlated Molecular Calculations. 3. The Atoms Aluminum Through Argon. *J. Chem. Phys.* **1993,** *98*, 1358-1371.
35. Aidas, K. *et al.*, The Dalton Quantum Chemistry Program System. *WIREs-Comput. Mol. Sci.* **2014,** *4*, 269-284.
36. Dalton, a Molecular Electronic Structure Program, Release v2019.alpha (2018), *see http://daltonprogram.org/.*

37. Becke, A. D., Density-Functional Thermochemistry .3. The Role of Exact Exchange. *J. Chem. Phys.* **1993,** *98*, 5648-5652.

38. Cronstrand, P.; Jansik, B.; Jonsson, D.; Luo, Y.; Ågren, H., Density Functional Response Theory Calculations of Three-Photon Absorption. *J. Chem. Phys.* **2004,** *121*, 9239-9246.

39. Friese, D. H.; Beerepoot, M. T. P.; Ringholm, M.; Ruud, K., Open-Ended Recursive Approach for the Calculation of Multiphoton Absorption Matrix Elements. *J. Chem. Theory Comput.* **2015,** *11*, 1129-1144.

40. Neely, R. K.; Magennis, S. W.; Dryden, D. T. F.; Jones, A. C., Evidence of Tautomerism in 2-Aminopurine from Fluorescence Lifetime Measurements. *J. Phys. Chem. B* **2004,** *108*, 17606-17610.

41. Stengel, G.; Purse, B. W.; Wilhelmsson, L. M.; Urban, M.; Kuchta, R. D., Ambivalent Incorporation of the Fluorescent Cytosine Analogues tC and tCo by Human DNA Polymerase alpha and Klenow Fragment. *Biochemistry* **2009,** *48*, 7547-7555.

42. Sholokh, M.; Improta, R.; Mori, M.; Sharma, R.; Kenfack, C.; Shin, D.; Voltz, K.; Stote, R. H.; Zaporozhets, O. A.; Botta, M.; Tor, Y.; Mely, Y., Tautomers of a Fluorescent G Surrogate and Their Distinct Photophysics Provide Additional Information Channels. *Angew. Chem. Int. Ed.* **2016,** *55*, 7974-7978.